ISSN 0030-400X, Optics and Spectroscopy, 2006, Vol. 100, No. 2, pp. 291–299. © Pleiades Publishing, Inc., 2006.
Original Russian Text © L.A. Ageev, E.D. Makovetskiĭ, V.K. Miloslavskiĭ, 2006, published in Optika i Spektroskopiya, 2006, Vol. 100, No. 2, pp. 328–336.

PHYSICAL OPTICS

Spontaneous S_- Gratings and Specific Features of Their Formation and Evolution in Photosensitive AgCl–Ag Films

L. A. Ageev, E. D. Makovetskiĭ, and V. K. Miloslavskiĭ

Kharkov National University, Kharkov, 61077 Ukraine

e-mail: evgeny.d.makovetsky@univer.kharkov.ua

Received February 22, 2005

Abstract—The formation and evolution of spontaneous S_- gratings in photosensitive waveguide AgCl–Ag films under the action of a laser beam are investigated experimentally and theoretically. It is found that in the cases of *s* and *p* polarizations of laser radiation these gratings differ significantly not only in the period but also in the structure and spatial and temporal stability. The different character of the gratings is explained in detail by the competition between the S_- gratings and other gratings evolving simultaneously in the film and the change in the scattering indicatrix in the case of *p* polarization as a result of intense evolution of degenerate *C* gratings. The regularity of S_- gratings on TM_0 modes in the case of *p* polarization and large angles of incidence makes it possible to increase the accuracy of determining the refractive indices of substrates using AgCl films corresponding to the cutoff thicknesses of TM_0 waveguide modes.

PACS numbers: 42.62

DOI: 10.1134/S0030400X06020214

INTRODUCTION

As is known [1, 2], spontaneous gratings are formed on surfaces of solids irradiated with a high-power laser beam. The reasons for this phenomenon are the interference of an incident wave (with a wavelength λ) with the surface TM modes excited as a result of the light scattering and the mass transfer in the interference field. At oblique incidence of an inducing beam, the type of a spontaneous grating depends on the beam polarization. In the case of linear *p* polarization, in a wide range of angles of incidence φ, so-called [3] S_- and S_+ gratings evolve with the following azimuthal angles α of the grating vectors: $\alpha = 0°$ and 180° (α is counted from the plane of incidence) and periods

$$d_{S_-, S_+} = \lambda/(1 \mp \sin\varphi). \quad (1)$$

These spontaneous gratings are dominant because, in the case of *p* polarization, scattered TM modes have the largest amplitude at $\alpha = 0°$ and 180°. The dominance of spontaneous S_- and S_+ gratings is confirmed by the calculation of the azimuthal dependence of the increment in their evolution due to positive feedback [4, 5]. However, the diffraction reflections in the given geometry are crescent-shaped rather than pointlike, which indicates the formation of S_- like gratings evolving on the modes with $\alpha \neq 0°$. It was ascertained in [3] that, irrespective of the type of the irradiated material, at $\varphi \gtrsim 35°$, spontaneous S_- and S_+ gratings are attenuated and disappear due to the evolution of regular degenerate *C* gratings. Periodic oscillations of the amplitudes of spontaneous S_- and S_+ gratings due to their competition in the nonlinear evolution stage were predicted theoretically in [6]. However, as far as we know, such oscillations have not been revealed experimentally.

Spontaneous gratings have also been found in photosensitive films with waveguide properties: Ag-doped AgCl films (AgCl–Ag) [7]; AgBr–Ag, AgI, and As_2S_3 films [8]; and photopolymer films [9]. Here, we will restrict our consideration to AgCl–Ag films since similar regularities in the evolution of spontaneous S_- and S_+ gratings have been observed for the films of other materials.

A thin AgCl film deposited on a transparent substrate (glass) is an asymmetric waveguide, in which both TE_m and TM_m modes can propagate [10]. However, these films are insensitive to visible light. To increase the film sensitivity, silver is incorporated into the film to precipitate as very small grains and form an absorption band peaked at 500 nm in the AgCl spectrum. Exposure of a film to a low-power gas laser beam leads to the excitation of waveguide modes in the film due to the light scattering by Ag grains. In the interference field formed by the incident wave and a scattered mode, silver mass transfer to the interference minima occurs, which finally leads to the formation of a quasiperiodic structure composed of microgratings (spontaneous grating domains). The mechanism of silver mass transfer was described in [7, 8]. In contrast to spontaneous gratings on surfaces of solids, evolution of spontaneous gratings on scattered TE and TM modes is possible in films. These gratings have different propagation constants depending on the photosensitive layer thick-

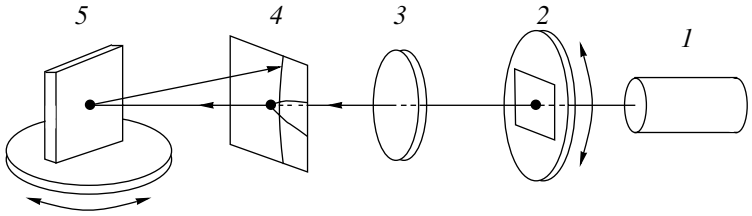

Fig. 1. Schematic diagram of the setup for generation and investigation of spontaneous gratings: (*1*) single-mode He–Ne laser (λ = 632.8 nm, P = 8 mW), (*2*) $\lambda/2$ plate on a vertical goniometer (for rotation of the plane of polarization), (*3*) collecting lens (F = 9.5 cm), (*4*) screen with an aperture for the laser beam, and (*5*) a sample on a horizontal goniometer.

ness; i.e., spontaneous gratings in photosensitive planar waveguides are characterized by a larger variety.

Spontaneous S_- and S_+ gratings were first found in thin ($h < h_{TM_0}$, where h_{TM_0} is the cutoff thickness of the TM_0 mode) AgCl–Ag films exposed to He–Ne [7] and He–Cd [11] laser radiation. Spontaneous gratings arose in the case of an *s*-polarized laser beam, exciting scattered TE_0 modes with periods similar to (1) in the film:

$$d_{S_-, S_+} = \lambda/(n_{\text{eff}} \mp \sin\varphi), \qquad (2)$$

where n_{eff} is the effective mode index (here, $n_{\text{eff}} = n_{TE_0}$). Then, the unusual dynamics of S_- and S_+ gratings was revealed [12]: spontaneous S_+ gratings, evolving in the initial stages of exposure, disappear with increasing exposure time and are replaced by S_- gratings. The competition of spontaneous S_- and S_+ gratings becomes especially pronounced when the laser beam is focused [13]. The pattern of anisotropic light scattering observed in the direction opposite to the incident beam direction exhibits a system of randomly arising, moving, and disappearing spots, which indicate the evolution of some microgratings and the disappearance of other microgratings (nonlinear optical turbulence). It was found that this turbulence is related to the evolution of spontaneous S_- gratings due to the suppression and elimination of S_+ gratings. The competition observed is somewhat like that predicted in [6]; however, instead of periodic oscillations (according to [6]), random oscillations of spots related to leaky modes with an average frequency decreasing with increasing exposure time were observed in [13].

We observed S_- gratings when a *p*-polarized beam was introduced into AgCl–Ag films with $h > h_{TM_0}$ either through a prism [8, 14] or from air (at large angles of incidence) [15]. Optical microscopy measurements [15] indicate a significant difference in the structure of S_{-, TE_0} and S_{-, TM_0} gratings. In this study, we performed a more detailed investigation of the formation and evolution of spontaneous S_- gratings in films exposed to *s*- and *p*-polarized laser beams to explain the difference noted.

EXPERIMENTAL TECHNIQUE

We studied spontaneous S_{-, TE_0} and S_{-, TM_0} gratings in AgCl–Ag films in the thickness range $h_{TM_0} \le h < h_{TE_1}$, where h_{TM_0}, and h_{TE_1} are the cutoff thicknesses of the corresponding modes:

$$h_{TM_0} = \frac{\lambda}{2\pi(n^2 - n_s^2)^{1/2}} \arctan\left[n^2 \frac{(n_s^2 - 1)^{1/2}}{(n^2 - n_s^2)^{1/2}} \right],$$

$$h_{TE_1} = \frac{\lambda}{2\pi(n^2 - n_s^2)^{1/2}} \arctan \frac{(n_s^2 - 1)^{1/2}}{(n^2 - n_s^2)^{1/2}} + \frac{\lambda}{2(n^2 - n_s^2)^{1/2}}, \qquad (3)$$

where λ = 632.8 nm is the He–Ne laser wavelength. The cutoff thicknesses h_{TM_0} = 94 nm and h_{TE_1} = 273 nm were calculated using the tabular values of $n = n_{AgCl}$ = 2.06 and n_s = 1.515 (glass). The photosensitive layer thickness was determined from the mass thickness calculated for the given geometry of material evaporation using a planar evaporator [16]. In addition, the photosensitive layer thickness was measured from the lines of equal monochromatic order by the Tolansky method [17]. AgCl–Ag films were deposited in vacuum on cold substrates by successive evaporation of AgCl and Ag. The mass thickness of Ag was about 10 nm, which determined the filling number for Ag films: $q \le 0.1$.

A schematic diagram of sample exposure is shown in Fig. 1. A narrow He–Ne laser beam (P = 8 mW, the mode waist width at the output mirror $w_0 = 3 \times 10^{-2}$ mm) passed through a quartz $\lambda/2$ plate mounted on a vertical goniometer. Then the beam passed through a collecting lens (F = 9.5 cm) and an aperture in a screen oriented perpendicularly to the beam direction, after which it fell on a sample mounted on a horizontal goniometer. At a distance of 60 mm between the laser and the lens, the width of the focused beam waist on the sample was w_F = 62 μm. The illuminated spot at $\varphi \ne 0°$ has an elliptical form with an area $S_F(\varphi) = S_F(0)\sec\varphi$, where $S_F(0) = 3 \times 10^3$ μm^2. The diffraction from spon-

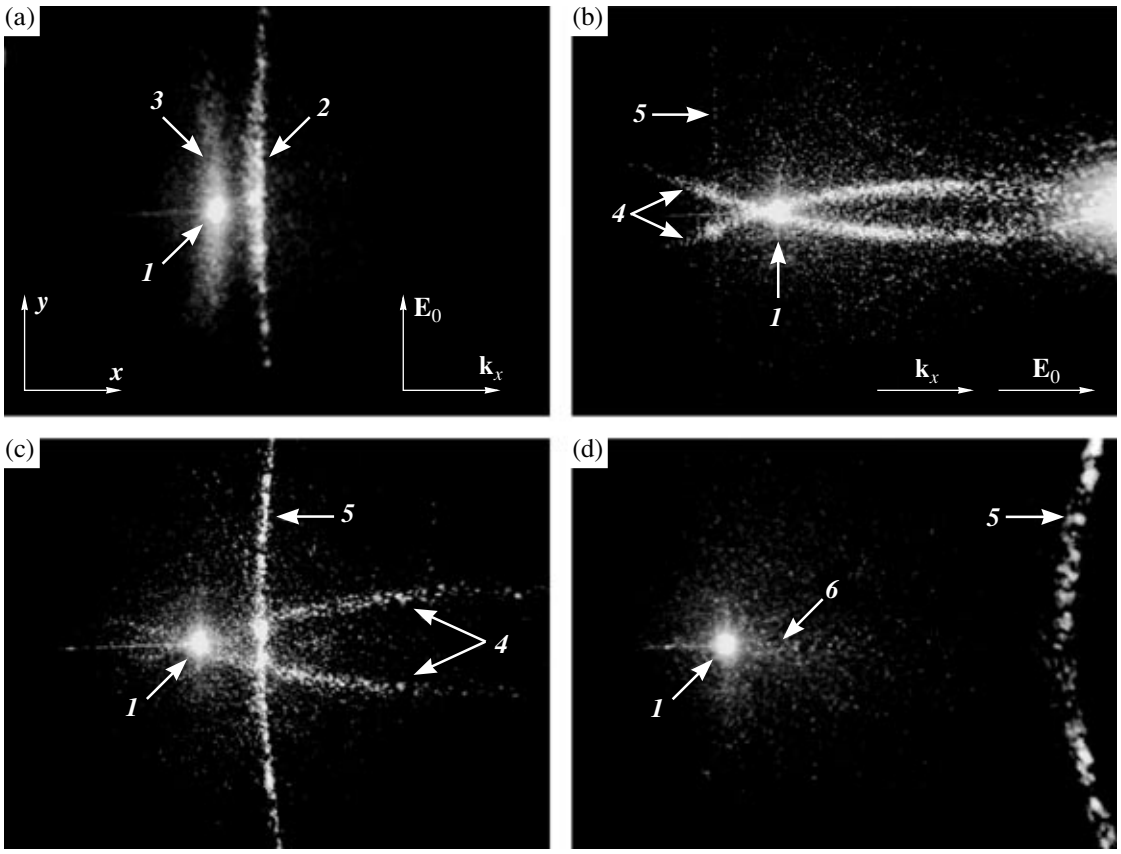

Fig. 2. Light scattering patterns on the screen (Fig. 1, *4*) during the exposure of an AgCl–Ag film: (a) *s* polarization, angle of incidence φ = 35°; (b) *p* polarization, φ = 25°; (c) *p* polarization, φ = 35°; and (d) *p* polarization, φ = 50°. Designations: (*1*) laser beam, (*2*) arc of diffraction of the laser beam to the order –1 by $S_{-,\,\mathrm{TE}_0}$-like gratings, (*3*) anisotropic scattering flame related to the diffraction of $S_{\mp,\,\mathrm{TE}_0}$ modes by $S_{\pm,\,\mathrm{TE}_0}$ gratings, (*4*) anisotropic scattering arcs related to the dominance of C_{TE_0} gratings, (*5*) arc of diffraction of the laser beam to the order –1 by $S_{-,\,\mathrm{TM}_0}$-like gratings, and (*6*) flame related to the existence of P_{TE_0}-like gratings.

taneous S_- gratings to the order $m = -1$ at $\varphi > \varphi^*$, where $\varphi^* = \arcsin[(n_{\mathrm{eff}} - 1)/2]$ (see [13]), was observed on the screen, which made it possible to investigate the spatial and temporal evolution of spontaneous S_- gratings during the exposure. Since n_{eff} changes from n_s to n, the least value $\varphi^* = 14°55'$ is obtained at $h = h_{\mathrm{TM}_0}$ and $n_{\mathrm{eff}} = n_{\mathrm{TM}_0} = n_s$. The periods of S_- gratings at different h and φ were measured by autocollimation. The required (*s* or *p*) polarization of the inducing beam was obtained by rotating the λ/2 plate. At $\varphi > 50°$, the periods of S_- gratings $d_{S_-} > \lambda$, which makes it possible to observe their spatial structure in an optical microscope (MII-4, observation in reflected light).

EXPERIMENTAL RESULTS

The patterns observed on the screen (Fig. 2; h = 100 nm; the exposure time t = 5 min; φ = 25°, 35°, and 50°) demonstrate a significant difference in the $S_{-,\,\mathrm{TE}_0}$ and $S_{-,\,\mathrm{TM}_0}$ gratings. In the case of *s* polarization, the diffraction reflection *2* from the $S_{-,\,\mathrm{TE}_0}$ grating (the order $m = -1$, Fig. 2a) is crescent-shaped and has a significant angular spread in the transverse (horizontal) direction. In addition, a small-angle anisotropic scattering reflection *3* (a so-called flame), intersecting the center of the laser beam *1*, is observed along the *y* axis, which is perpendicular to the plane of incidence. The patterns obtained at φ = 25° and 50° are not shown here since they do not differ qualitatively. They also demonstrate a flame and a crescent-shaped reflection corresponding to the diffraction to the order $m = -1$. The position of the reflection *2* depends on φ: at φ < 33°, it is located on the left of the beam *1*. With an increase in φ, the reflection *2* shifts to $\mathbf{k}_x$ (here, $\mathbf{k}_x = \mathbf{i}(2\pi/\lambda)\sin\varphi$ is the component of the wave vector of the laser beam that is parallel to the photosensitive layer); crosses the center of the beam *1*; and, at φ > 33°, is located on the right

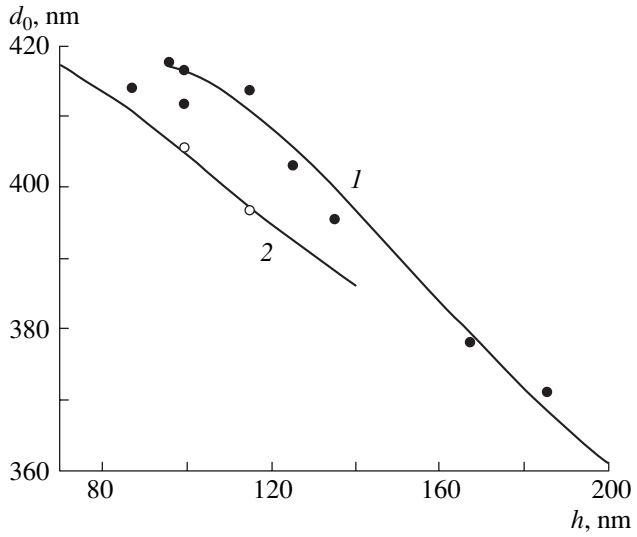

Fig. 3. Dependences of d_0 on the thickness h of AgCl films ($d_0 = \lambda/n_{\text{eff}}$). Filled circles and the black curve show, respectively, the experimental values and the results of calculation by the dispersion equation for TM_0 gratings ($n_{\text{eff}} = 2.12$). Open circles and the gray curve show the same for TE_0 gratings ($n_{\text{eff}} = 1.94$).

of the beam (Fig. 2a). The intensity of the reflection *2* does not change.

In the case of *p* polarization, the patterns obtained at different φ are significantly different. At φ < 25°, the vertical diffraction reflection is absent; i.e., $S_{-,\,TM_0}$ gratings are not formed (Fig. 2b). However, one can see two anisotropic scattering arcs *4*, passing through the centers of the initial and reflected beams. It will be shown below that the appearance of the arcs *4* is related to the formation of dominant C_{TE_0} gratings. At φ = 35° (Fig. 2c), the reflection *5* corresponding to the diffraction to the order $m = -1$ can be clearly seen simultaneously with the attenuation of the arcs *4* from the *C* gratings. At the points of intersection of the arcs *4* and *5* (Figs. 2b, 2c), a significant increase in brightness is observed, which corresponds to the enhancement of certain S_--like gratings. The reasons for this enhancement were discussed in [18]. At φ = 50° (Fig. 2d), the arcs *4* disappear and a weak scattering reflection *6* extended along the $\mathbf{k}_x$ axis becomes pronounced. This scattering reflection exists at all values of φ; however, it is weak against the background of the bright arcs *4*. At the same time, the scattering reflection extended along the *y* axis is absent at all values of φ. Measurement of the periods of S_- gratings in the two polarizations gives $d_s = 560$ nm and $d_p = 660$ nm at φ = 35°. These results, according to (2) and the calculation of n_{eff} by the dispersion equations [10], indicate the formation of gratings in the cases of *s* and *p* polarizations on the TE_0 and TM_0 modes, respectively.

The time evolution of different S_- gratings is also different. With an increase in the exposure time, the diffraction reflection *2* from TE_0 gratings shifts significantly in the $\mathbf{k}_x$ direction, which indicates an increase in the period of the spontaneous TE_0 gratings with time. In this case, the angular width of the reflection narrows from several degrees to 30′. In the initial stage of exposure, the flame *3* demonstrates a strong optical turbulence. With increasing exposure time, the frequency of random oscillations of spots in the pattern decreases and the small-angle scattering reflection *3* in the counterpropagating beam decreases to complete disappearance. These results are similar to those obtained in [13], where this character of evolution was explained.

The character of the evolution of the reflection *5* from $S_{-,\,TM_0}$ gratings is different: long-term exposure does not lead to a significant shift or change in the half-width of this reflection; only its length slightly decreases.

The dependences of the periods *d* on the film thickness *h* for the $S_{-,\,TE_0}$ and $S_{-,\,TM_0}$ gratings were measured at φ = 40° in the range of *h* from 70 to 180 nm, which corresponds to the existence of TE_0 and TM_0 modes. Since the period of $S_{-,\,TE_0}$ gratings depends on the exposure time, we measured the limiting values of *d* obtained at long exposure times. Figure 3 shows the values $d_0 = \lambda/n_{\text{eff}}$, where $d_0 = d[1 + (d/\lambda)\sin\varphi]^{-1}$. A systematic decrease in d_0 with increasing *h* is observed. Figure 3 also shows the dependences $d_0(h)$ calculated by the dispersion equations. The calculation method is considered below.

The micrographs in Fig. 4 were obtained at φ = 70° since the periods of spontaneous S_- gratings are much larger than λ at this angle of incidence (the observation and photographing were performed in white light). The illuminated spot had the form of an ellipse extended in the $\mathbf{k}_x$ direction, with axes of 60 and 170 μm (Fig. 4c). A portion of the spot with an area of 80×60 μm^2 near the spot center was photographed. One can see a significant difference in the spontaneous $S_{-,\,TE_0}$ and $S_{-,\,TM_0}$ gratings not only in periods but also in shape.

On the whole, the quasi-periodic structure of spontaneous $S_{-,\,TE_0}$ gratings (Fig. 4a) consists of individual small microgratings extended in the $\mathbf{k}_x$ direction, with an average number of lines of about 10–15. Some microgratings are up to 10 μm in length and 3 μm in width. The vectors **K** of the microgratings have a spread with respect to the dominant direction, perpendicular to $\mathbf{E}_0$; they are separated by fairly wide bright areas, where their evolution is significantly reduced. The microgratings are poorly matched with each other in phase.

The quasi-periodicity of the structure of $S_{-,\,TM_0}$ gratings (Fig. 4b) is more pronounced. In the middle of the

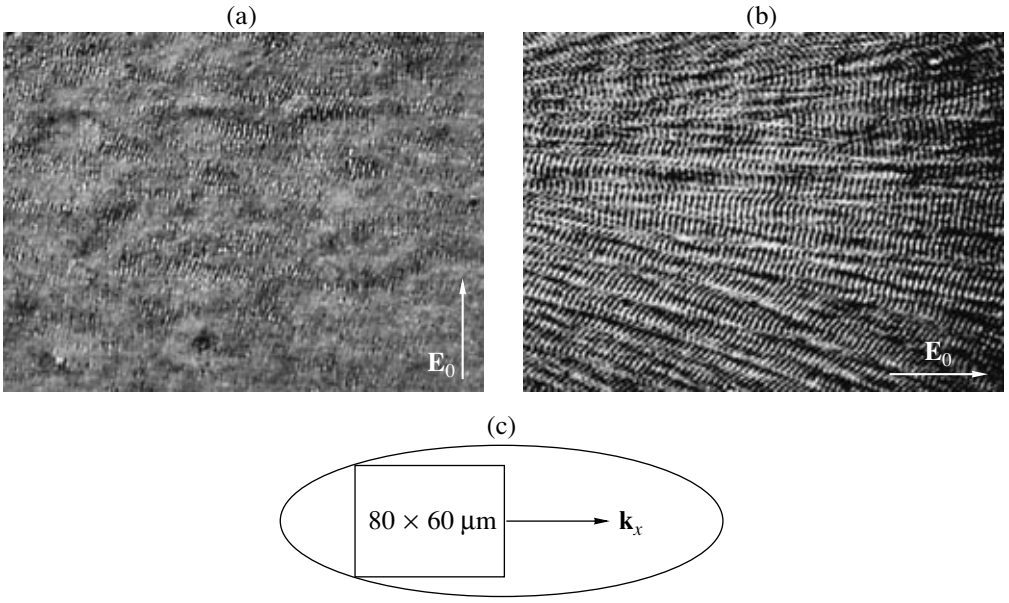

Fig. 4. Micrographs of spontaneous gratings obtained in an MII-4 optical microscope in reflected white light. The gratings were formed at an angle of incidence $\varphi = 70°$ in (a) *s* polarization ($S_{-,\,\mathrm{TE}_0}$-like gratings can be seen) and (b) *p* polarization ($S_{-,\,\mathrm{TM}_0}$-like gratings can be seen); (c) the position of the portion of the irradiated spot that was photographed.

illuminated spot, some micrograting have the form of narrow, often lancet-shaped, bands, which are significantly extended in the $\mathbf{k}_x$ direction. Neighboring micrograting are separated by narrow bright bands of about 1 μm in size. The number of lines of the micrograting varies from 20 to 30; their vectors **K** are oriented predominantly parallel to $\mathbf{E}_0$. The length of some lancet-shaped micrograting reaches 30 μm and their width in the middle region is 3–5 μm. At the edges of the photograph, close to the transverse boundaries of the illuminated spot, the micrograting axes deviate from the plane of incidence by 10°–20°, with increasing tilt angle as the micrograting approach the boundaries. In addition, in contrast to the central region of the spot, the grating lines on the periphery are not perpendicular to the grating axes. Also, the period of spontaneous gratings at the spot periphery decreases on average to 0.9 with respect to the period in the central area of the spot.

DISCUSSION

To establish the conditions for the evolution of spontaneous S_- gratings on scattered TE_0 and TM_0 modes, one has to know the indicatrices of scattered radiation. Generally, these indicatrices in a waveguide film are rather complicated. They change during the formation and evolution of spontaneous gratings due to the redistribution of Ag grains, which are the main scattering centers in AgCl–Ag films. Here, we will restrict ourselves to a simple case: light is scattered by small spherical Ag grains with a diameter much smaller than λ (about 10 nm). At a small filling number of the initial film ($q \le 0.1$), we can neglect the multiple scattering and consider one-particle scattering. In this case, the indicatrices can be calculated using the conventional theory of scattering by small particles [19], with the 4×4 Müller matrix. Since we are interested in the angular distribution of the scattered light intensity, we do not take into account its radial distribution in the waveguide layer. Determination of the radial distribution is an independent problem [20, 21].

For an *s*-polarized incident beam (the polarization vector $\mathbf{E}_0 \parallel y$ lies in the plane (x, y) of the photosensitive layer), the angular intensity distribution of the light scattered to the TE and TM modes in the far zone is

$$I_{s,\,\mathrm{TE}} \propto \cos^2\alpha, \quad I_{s,\,\mathrm{TM}} \propto \sin^2\alpha\cos^2\theta, \qquad (4)$$

where α and θ are, respectively, the azimuthal and meridional angles determining the scattering direction: $\alpha = \angle(\boldsymbol{\beta}, x)$, $\theta = \angle(\mathbf{k}_s, z)$ (the z axis is perpendicular to the photosensitive layer); $\mathbf{k}_s$ is the wave vector of the scattered wave; and $\boldsymbol{\beta}$ is the wave vector of the excited mode (equal to the tangential component $\mathbf{k}_s$). It follows from (4) that the scattering to the TE mode depends only on α and is maximum at $\alpha = 0, \pi$. The intensity of light scattered to the TM mode is highest at $\alpha = \pm\pi/2$ and depends on θ. In our case, the angle θ is fixed and related to the propagation constant of the TM mode by the expression [10]

$$\beta_{\mathrm{TM}} = k_0 n_{\mathrm{TM}} = k_0 n \sin\theta,$$

where $k_0 = 2\pi/\lambda$.

For a *p*-polarized incident beam ($\mathbf{E}_0$ is in the plane of incidence (x, z)), the angular distribution of scattered light is set by the relations

$$I_{p,\mathrm{TE}} \propto \sin^2\alpha\cos^2\psi,$$
$$I_{p,\mathrm{TM}} \propto (\cos\alpha\cos\theta\cos\psi + \sin\theta\sin\psi)^2, \quad (5)$$

where ψ is the angle of refraction of the beam in the film. In contrast to the case of *s* polarization, the intensity of scattered light depends on the angle of incidence since $n_0\sin\varphi = n\sin\psi$, where n_0 is the refractive index of the medium surrounding the photosensitive layer on the glass plate.

Indicatrices (4) and (5) determine the dominance of particular spontaneous gratings in the initial stage of their formation. In the case of *s* polarization, $S_{-,\mathrm{TE}}$ and $S_{+,\mathrm{TE}}$ gratings are the dominant ones ($\alpha = 0$ or π). In the case of *p* polarization, so-called parquet (*P*) gratings [11], evolving on scattered TE modes at $\alpha = \pm\pi/2$, and $S_{-,\mathrm{TM}}$ and $S_{+,\mathrm{TM}}$ gratings ($\alpha = 0°$, $\theta > 0$ and $\alpha = 180°$, $\pi/2 < \theta < \pi$, respectively) can be considered to be dominant. In this case, the dependences of $I_{p,\mathrm{TE}}$ and $I_{p,\mathrm{TM}}$ on the angle of incidence can be used to determine the result of the competition of the $S_{-,+}$ and *P* gratings.

At $\varphi \neq 0°$, the dominance of gratings is determined not only by the indicatrices (4) and (5). Let us consider the diffraction from plane spontaneous gratings forming during illumination of a sample by a laser beam. In this case, the tangential component $\mathbf{k}_d$ of a diffracted wave is

$$\mathbf{k}_d = \mathbf{k}_x + m\mathbf{K}(\alpha)$$
$$= [k_x + m(\beta\cos\alpha - k_x)]\mathbf{i} + m\beta\sin\alpha\mathbf{j}, \quad (6)$$

where $\mathbf{K}(\alpha)$ is the vector of a plane grating formed on the waveguide mode scattered at an azimuthal angle α; $m = \pm1, \pm2 \ldots$ is the diffraction order; and $\mathbf{i}$ and $\mathbf{j}$ are the unit vectors of the x and y axes, respectively. For the order $m = 1$, we have $\mathbf{k}_d = \boldsymbol{\beta}$; i.e., the grating introduces a mode whose interference with the incident beam causes the evolution of this mode. Thus, all spontaneous gratings evolve as a result of positive feedback. However, if $m = -1$ in (6), $k_{dx} = 2k_x - \beta\cos\alpha$ and, generally, $\mathbf{k}_d \neq \boldsymbol{\beta}$. At $m = -1$, the diffraction may excite leaky modes into air (if $k_d < k_0$), leaky modes into the substrate (if $k_0 < k_d < k_0 n_s$), and evanescent modes (if $k_d > k_0 n_s$).

The only exception is the azimuthal angles

$$\alpha^* = \pm\arccos(k_x/\beta). \quad (7)$$

At $\alpha = \alpha^*$, diffraction to the orders $m = \pm1$ introduces waveguide modes on which degenerate *C* gratings [3, 5] with antiparallel vectors $\mathbf{K} = \pm(\beta^2 - k_x^2)^{1/2}\mathbf{j}$ are formed. Since *C* gratings evolve on double Wood anomalies (i.e., waves of two diffraction orders propagate along the grating), the increment in their evolution is much larger than the increment of spontaneous gratings evolving at azimuthal angles close to α^* [5, 22]. This circumstance determines the regularity of *C* gratings.

Figure 5 shows the dependence of the relative intensities of scattered light on the angle of incidence of a laser beam (formulas (4) and (5)) for the azimuthal angles $\alpha = 0$, $\pi/2$, and α^*, corresponding to the formation of dominant S_-, *P*, and *C* gratings. The calculation was performed at the same values $n_{\mathrm{AgCl}} = 2.06$ and $n_s = 1.515$ at which the cutoff thicknesses of the waveguide modes (3) were determined above and at the values $n_{\mathrm{TE}_0} = 1.63$ and $n_{\mathrm{TM}_0} = 1.52$, corresponding to the experimental conditions.

It can be seen from Fig. 5a that, in the case of *s* polarization, S_{-,TE_0} and S_{+,TE_0} gratings should be dominant at all values of φ, which is consistent with the experimental data (Fig. 2a). In the case of *p* polarization, the situation is different (Fig. 5b). At $\varphi < 40°$, the scattering to the TE_0 mode at $\alpha = \pm\pi/2$ or $\alpha = \alpha^*$ is dominant. However, with increasing φ, the intensity of scattering to the TM_0 mode at $\alpha = 0$ increases, whereas the intensity of scattering to the P_{TE_0} modes at $\alpha = \pm\pi/2$ or α^* decreases. In addition, according to (7), α^* decreases with increasing φ, which leads to a decrease in the intensities of the modes of *C* gratings even when the scattering indicatrix does not vary with φ. Thus, at $\varphi < 40°$, the *C* and *P* gratings on TE_0 modes should prevail, while, at $\varphi > 40°$, S_{-,TM_0} gratings should be dominant. This analytical result is in qualitative agreement with the experiment: the diffraction reflection *5* with $m = -1$ from S_{-,TM_0} gratings at $\varphi = 25°$ (Fig. 2b) can hardly be seen, whereas, at $\varphi = 35°$ (Fig. 2c), its intensity is high and increases with increasing φ.

Due to the short period of *C* and *P* gratings, diffraction from these gratings to the order –1 is not observed. However, their existence is confirmed by the anisotropic scattering patterns on the screen. Anisotropic (small-angle) scattering, as was shown in [8], is the result of the diffraction of waveguide modes excited on the dominant gratings with the vector $\mathbf{K}_0$ and on the neighboring gratings with the vector $\mathbf{K}$ only slightly differing from $\mathbf{K}_0$. In this case, leaky modes arise (leading to the occurrence of flames on the screen) with the tangential (in the layer plane) components

$$\mathbf{k}_r = \boldsymbol{\beta}_0 + m\mathbf{K}(\alpha)$$
$$= [\beta\cos\alpha_0 + m(\beta\cos\alpha - k_x)]\mathbf{i} \quad (8)$$
$$+ (\beta\sin\alpha_0 + m\beta\sin\alpha)\mathbf{j},$$

where $\boldsymbol{\beta}_0$ is the wave vector of the dominant mode, α_0 is its azimuthal angle, α is the azimuthal angle of the waveguide mode forming a neighboring grating, and $m = \pm1$. According to (8), for the values of the parameters $m = 1$; $\alpha_0 = 0, \pi$; and $\alpha = \pi, 0$ (diffraction of a mode

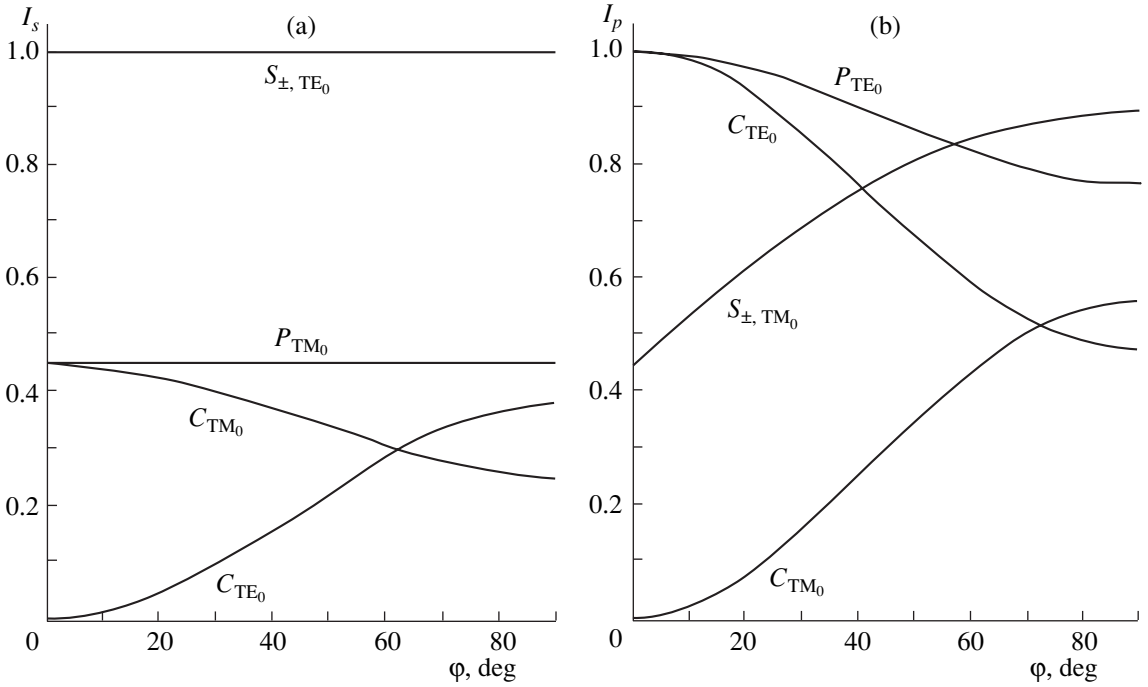

Fig. 5. Dependences of the relative intensities of scattered TE_0 and TM_0 modes on the angle of incidence of a laser beam: (a) *s*-polarized beam, formulas (4), and (b) *p*-polarized beam, formulas (5). For the film with $n_{AgCl} = 2.06$ on a substrate with $n_s = 1.515$ in air, $n_{TE_0} = 1.63$, $n_{TM_0} = 1.52$, and $\theta = 48°$ for TM_0 modes. The curves for the $S_\pm$ gratings (azimuthal angles of the modes $\alpha = \pi, 0$) and *P* gratings ($\alpha = \pi/2$) evolving on ordinary Wood anomalies and for the C_{TE_0} and C_{TM_0} gratings azimuthal angles of the modes α^* depend on φ, see formula (7)) are shown.

from an S_- grating on an S_+ grating, and vice versa), $\mathbf{k}_r = -k_x\mathbf{i}$; i.e., a leaky mode arises in the direction opposite to the laser beam direction. At $\alpha_0 = 0, \pi$ and α only slightly differing from either 0 or π, the spots from leaky modes appearing on the screen form anisotropic scattering arcs extended along the *y* axis. The tangents to these arcs at the point on the laser beam path corresponding to $\mathbf{k}_r = -k_x\mathbf{i}$ are parallel to the *y* axis. Thus, in the case of *s* polarization, the scattering related to the penetration of $S_{\mp, TE_0}$ modes to neighboring $S_{\pm, TE_0}$ gratings is observed on the screen. This scattering is accompanied by turbulence and gradual disappearance of S_+ gratings (see [13] for details).

In the case of *p* polarization, the anisotropic scattering arcs *4* (Figs. 2b, 2c) are related to the dominant C_{TE_0} gratings, for which $\boldsymbol{\beta}_0 = k_x\mathbf{i} \pm (\beta^2 - k_x^2)^{1/2}\mathbf{j}$. At $m = 1$, the tangents to the arcs at the point $\mathbf{k}_r = -k_x\mathbf{i}$ are tilted to the plane of incidence at an angle of $\mp\sin\varphi(n_{TE_0}^2 - \sin^2\varphi)^{-1/2}$; i.e., the convergence of the arcs *4* increases with increasing φ. In addition, these arcs weaken with increasing φ and disappear completely at $\varphi > 45°$, which indicates indirectly the disappearance of C_{TE_0} gratings. However, at $\varphi = 50°$, the anisotropic scattering at small angles to the plane of incidence increases significantly (Fig. 2d, the flame *6*). We assign this scattering to the dominant *P* gratings formed on TE_0 modes with $\boldsymbol{\beta}_0 \neq \pm\beta\mathbf{j}$. In this case, the mean tangent to the arcs (at the point where they intersect the laser beam) lies in the plane of incidence. The anisotropic scattering spread is related to the irregularity of the *P* gratings. Thus, the results of the analysis of the patterns on the screen are implicitly in agreement with the calculation of the intensity of the radiation scattered to the modes generating S_{-, TM_0}, P_{TE_0}, and C_{TE_0} gratings. At the same time, the absence of the vertical flame characteristic of the *s* polarization of the laser beam at all φ indicates the absence of S_{+, TM_0} gratings at all exposure times.

The absence of these gratings may be caused by the existence of C_{TE_0} or P_{TE_0} gratings at large φ. As the electron micrographs show [11], the lines from regular C_{TE_0} gratings are formed by individual silver grains extended in the k_x direction. In the case of incidence of *p*-polarized light, along with TE_0 modes, which facilitate the evolution of C_{TE_0} gratings, light scattering from individual lines occurs. In the first-order approximation, a chain of extended grains forming a line can be approximated by a cylinder with a permittivity different

from that of AgCl, oriented parallel to the x axis. When the vector of the electric field of the incident beam lies in the plane of incidence (p polarization), the front of the wave scattered from the cylinder has the form of a cone moving along the line axis in the far zone [19]. The wave vector of scattered light (normal to the plane that is tangent to the cone at a given point) always has a component $\mathbf{k}_{sx} = k_x\mathbf{i}$ at any azimuthal angle α. Thus, at $\alpha = 0$, scattering to the TM_0 mode along the $\mathbf{k}_x$ direction occurs. This scattering facilitates the evolution of spontaneous S_{-,TM_0} gratings and impedes the formation of spontaneous S_{+,TM_0} gratings. In the case of s polarization, C gratings are not formed, which leads to equiprobable scattering of TE_0 modes at azimuthal angles $\alpha = 0$ and π. This circumstance leads to competition between the spontaneous S_{-,TE_0} and S_{+,TE_0} gratings. At $\varphi > 45°$, in the case of p polarization, C_{TE_0} gratings vanish; however, irregular P gratings arise, whose lines are inclined at angles of 20°–30° and –20° to –30° to the plane of incidence. The relatively small angle of inclination of these gratings also facilitates scattering of TM_0 modes at azimuthal angles α close to 0, i.e., the preferred evolution of spontaneous S_{-,TM_0} gratings (Fig. 2d).

It is now clear why the structures in the photographs of portions of spontaneous S_{-,TE_0} and S_{-,TM_0} gratings in Figs. 4a and 4b differ radically. The small length of S_{-,TE_0} gratings and large gaps between them are the result of their competition during evolution with S_{+,TE_0} gratings, which fill these gaps and cannot be resolved in an optical microscope because of their very short periods. At the same time, the absence of S_{+,TE_0} gratings in the case of p polarization facilitates a freer evolution of S_{-,TM_0} microgratings in the $\mathbf{k}_x$ direction. The microgratings have a large length in the $\mathbf{k}_x$ direction, which is limited only by their competition with neighboring microgratings evolving in the same direction but formed at other scattering centers. As was mentioned above, the diffraction reflection from spontaneous S_{-,TE_0} gratings shifts in the $\mathbf{k}_x$ direction with increasing exposure time due to an increase in the period of S_{-,TE_0} gratings. This effect was revealed for S_{-,TE_0} gratings in [13] and studied in detail in [23] for AgCl–Ag films at normal incidence of the inducing beam with λ = 633 nm. It was ascertained in [23] that, before the formation of spontaneous gratings, the refractive index of a composite AgCl–Ag film, due to the presence of a strong colloidal absorption band of Ag at 500 nm, exceeds the value of n_{AgCl} and becomes as high as 2.4 at λ = 633 nm and $q \simeq 0.3$. With an increase in the exposure time, the period increases by a factor of 1.25 due to a decrease in n. The reason for this phenomenon is as follows: during the formation of spontaneous gratings, silver precipitates in minima of the interference field, and the effective exponent of the TE_0 mode is determined primarily by the refractive index in the interference maxima, which tend to be free of silver. The values of $d_0 = \lambda/n_{eff}$ shown in Fig. 3 were obtained at long exposure times (1 h or more). The value of n_{eff} found by the dispersion equation was used to calculate the dependence $d_0(h)$, which is in good agreement with experiment at n = 1.94. The smaller value of n in comparison with n_{AgCl} = 2.06 is related to the porosity of AgCl films in interference maxima, caused by the dissolution of Ag grains in the lines of spontaneous S_{+,TE_0} gratings and their precipitation in the lines of spontaneous S_{-,TE_0} gratings.

At the same time, similar calculation of $d_0(h)$ for spontaneous S_{-,TM_0} gratings gives the best agreement with experiment at n = 2.12. In our case, in contrast to [23], the filling number for a film containing silver is $q \simeq 0.1$, which yields (at λ = 633 nm) a refractive index of the initial film equal to 2.18. The small difference in n before and after the exposure indicates the conservation of Ag grains in the maxima of interference of TM_0 modes with the incident beam and explains the absence of a significant shift of diffraction reflections from spontaneous S_{-,TM_0} gratings during the exposure. Simultaneous existence of C_{TE_0} and P_{TE_0} gratings is the reason for the small variation in n.

At a fixed exposure time, the period of spontaneous gratings depends on the laser beam intensity. This fact was established in [23] in measuring the radial dependence of the period of spontaneous gratings upon illumination by an extended Gaussian beam. A significant decrease in the period of TE_0 gratings and, accordingly, an increase in n with increasing distance from the beam center were revealed. The increase in n at the periphery of the waist of a focused Gaussian beam was explained by the inclination of the axes of S_{-,TM_0} microgratings and the decrease in their period (Fig. 4b). Indeed, on the slope of the Gaussian beam intensity, where the derivatives $|dI/dy|$ and dn/dy have the largest values, a TM_0 mode propagating along peripheral regions will shift to the beam periphery due to refractive index gradient.

CONCLUSIONS

An analysis of the formation and evolution of spontaneous S_- gratings under the action of s- and p-polarized laser beams revealed a significant difference between the gratings not only in the period but also in the structure and the spatial and temporal stability. The evolution of S_{-,TE_0} gratings in the case of s polarization is controlled by their competition with S_{+,TE_0} gratings, which determines their instability during the film expo-

sure, whereas the evolution of S_{-,TM_0} gratings in the case of p polarization depends on the existence of C_{TE_0} and P_{TE_0} gratings. At all angles of incidence of a p-polarized beam, S_{+,TM_0} gratings are absent, which leads to a better stability and structure of S_{-,TM_0} gratings in comparison with S_{-,TE_0} gratings. As was shown in [24], the use of S_- gratings formed at the cutoff thicknesses of TE_0 modes makes it possible to determine with a high accuracy the refractive indices of substrates in a wide range (up to 2.5). The better structure of S_{-,TM_0} gratings, which manifests itself in narrower diffraction reflections and better stability, makes it possible to increase the accuracy in determining the refractive index n of substrates using AgCl films formed at the cutoff thicknesses of waveguide TM_0 modes.

REFERENCES

1. A. E. Siegman and P. M. Fauchet, IEEE J. Quantum Electron. **QE-22** (8), 1384 (1986).
2. A. M. Bonch-Bruevich, M. N. Libenson, V. S. Makin, and V. V. Trubaev, Opt. Eng. **31** (4), 718 (1992).
3. J. F. Young, J. S. Preston, H. M. van Driel, and J. E. Sipe, Phys. Rev. B **27** (2), 1155 (1983).
4. P. S. Kondratenko and Yu. N. Orlov, Kvantovaya Élektron. (Moscow) **14** (5), 1038 (1987) [Sov. J. Quantum Electron. **17**, 659 (1987)].
5. R. V. Arutyunyan, V. Yu. Baranov, L. A. Bol'shov, D. D. Malyuta, and A. Yu. Sebrant, *Action of Laser Radiation on Materials* (Nauka, Moscow, 1989) [in Russian].
6. L. A. Bol'shov, A. V. Moskovchenko, and M. I. Persiantsev, Zh. Éksp. Teor. Fiz. **94** (4), 62 (1988) [Sov. Phys. JETP **67**, 683 (1988)].
7. L. A. Ageev and V. K. Miloslavskiĭ, Zh. Tekh. Fiz. **54** (5), 888 (1984) [Sov. Tech. Phys. **29**, 530 (1984)].
8. L. A. Ageev and V. K. Miloslavsky, Opt. Eng. **34** (4), 960 (1995).
9. P. E. Dyer and R. J. Farley, J. Appl. Phys. **74** (2), 1442 (1993).
10. M. Adams, *An Introduction to Optical Waveguides* (Wiley, New York, 1981; Mir, Moscow, 1984).
11. V. B. Blokha, L. A. Ageev, and V. K. Miloslavskiĭ, Zh. Tekh. Fiz. **85** (10), 1967 (1985) [Sov. Tech. Phys. **30**, 1154 (1985)].
12. M. V. Varminsky, L. A. Ageev, and V. K. Miloslavsky, J. Opt. **29**, 253 (1998).
13. L. A. Ageev, V. K. Miloslavskiĭ, and E. I. Larionova, Opt. Spektrosk. **89** (6), 1032 (2000) [Opt. Spectrosc. **89**, 955 (2000)].
14. V. K. Miloslavsky, L. A. Ageev, and V. I. Lymar, Proc. SPIE **1440**, 90 (1990).
15. L. A. Ageev, M. V. Pogrebnyak, and V. K. Miloslavskiĭ, Opt. Spektrosk. **97** (2), 346 (2004) [Opt. Spectrosc. **97**, 325 (2004)].
16. V. V. Slutskaya, *Thin Films in Microwave Technique* (Gosénergoizdat, Moscow, 1962) [in Russian].
17. *Physics of Thin Films: Advances in Research and Development*, Ed. by G. Hass and R. E. Thun (Academic, New York, 1967; Mir, Moscow, 1970).
18. E. D. Makovetsky and V. K. Miloslavsky, Opt. Commun. **244**, 445 (2005).
19. C. F. Bohren and D. R. Huffman, *Absorption and Scattering of Light by Small Particles* (Wiley, New York, 1983; Mir, Moscow, 1986).
20. S. R. J. Brueck, IEEE J. Sel. Top. Quantum Electron. **6** (6), 899 (2000).
21. V. I. Lymar, Acta Phys. Pol. A **103** (2–3), 275 (2003).
22. V. K. Miloslavsky, E. D. Makovetsky, and L. A. Ageev, Opt. Commun. **232**, 303 (2004).
23. V. I. Lymar', V. K. Miloslavskiĭ, and L. A. Ageev, Opt. Spektrosk. **83** (6), 995 (1997) [Opt. Spectrosc. **83**, 921 (1997)].
24. L. A. Ageev, V. K. Miloslavskiĭ, and O. V. Tyutyunnik, Zh. Prikl. Spektrosk. **68** (2), 147 (2001).

Translated by Yu. Sin'kov